

## ORIGINAL ARTICLE

# Enhanced dielectric behavior in nanocomposites of polyurethane bonded with copper phthalocyanine oligomers

Jingwen Wang, Congcong Wu, Ruonan Liu and Shuqin Li

To increase the electric energy density of dielectric elastomers, high dielectric constant nanocomposites were developed by chemically bonding oligomers of copper phthalocyanine oligomers (CuPc), a high dielectric constant organic semiconductor, to polyurethane (PU). Transmission electron microscope (TEM) images revealed that the sizes of the CuPc particles in the nanocomposite of PU functionalized with 8.78 vol% of CuPc were in the range of 10–20 nm, much smaller than the sizes (250–600 nm) in PU blended with the same volume fraction of CuPc. At 100 Hz, the nanocomposite film exhibited a dielectric constant of 391, representing a more than 60-fold increase with respect to pure PU. The enhanced dielectric response in the nanocomposite makes it possible to induce a high electromechanical response. A strain of 17.7% and an elastic energy density of  $0.927 \text{ J cm}^{-3}$  were achieved under an electric field of  $10 \text{ V } \mu\text{m}^{-1}$ .

*Polymer Journal* (2014) 46, 285–292; doi:10.1038/pj.2013.101; published online 29 January 2014

**Keywords:** dielectric elastomer; dielectric properties; microstructure; nanocomposite; polyurethane

## INTRODUCTION

Electroactive polymers (EAPs) capable of responding to external electrical stimulation by undergoing significant size or shape changes have attracted increasing interest over the past few decades because of their unique properties, including light weight, flexibility, ease of processing over large areas, conformability to complex shapes and surfaces and low cost.<sup>1–6</sup> According to their operational mechanism, EAPs can be divided into two main classes: ionic EAPs, which are activated by the electrically induced transport of ions in a liquid medium, and electronic EAPs, which are activated by electric fields or Coulomb forces. The former generally require low voltages but high currents, while the latter need high voltages but low currents.<sup>6</sup> Among electronic EAPs, dielectric elastomers (DEs) and various actuators developed with them have been intensely studied in the past decade.

A DE actuator consists of a polymer film sandwiched between two compliant electrodes (Figure 1). When a voltage is applied, the elastomer film decreases in thickness and expands in area, converting electrical energy into mechanical energy. This field of study is growing rapidly, as measured by the number of research papers, the performance of the technology and the diversity of potential applications, including micropumps, energy harvesters, space robotics, positioners and bioinspired robotic systems. This growth is because of the many attractive features of DE actuators, including their large

strain, fast response, high efficiency, high power-to-mass ratio, facile processability and affordability.<sup>1–7</sup> In earlier years, much of the research focus was on actuator configurations, while in more recent years, the focus has turned to investigating material properties that are critical to enhancing actuator performance. The further development of DEs as a viable actuator technology will require further effort, and many exciting challenges lie ahead. One of the major challenges in the development of DE actuators is meeting the high electric field requirement. Driving voltages of up to  $150 \text{ MV m}^{-1}$  are required to actuate these elastomeric films because the dielectric constants of the elastomers, such as polyurethane (PU), acrylic resin and polydimethylsiloxane, are low ( $<7.0$ ).<sup>3,6,8</sup> As a result, these polymers usually require high electric fields to generate a high elastic energy density, which limits their applications, particularly in the biomedical fields.

In recent years, polymer-based nanocomposites with chemically bonded or blended nanoparticles have been studied extensively. These composite materials, consisting of building blocks on the scale of nanometers or tens of nanometers, exhibit improved physical properties. Composite methods, in which high dielectric constant particulates (such as ferroelectric ceramics) are added to a polymer matrix, have been developed to fabricate high dielectric constant polymeric composites.<sup>3,9</sup> Dielectric fillers increase the dielectric response of polymeric materials, allowing the field required to

Department of Materials Science and Engineering, College of Materials Science and Technology, Nanjing University of Aeronautics and Astronautics, Nanjing, People's Republic of China

Correspondence: Dr J Wang, Department of Materials Science and Engineering, College of Materials Science and Technology, Nanjing University of Aeronautics and Astronautics, 29 Yudao Street, Nanjing 210016, People's Republic of China.

E-mail: wjw\_msc@nuaa.edu.cn

Received 13 October 2013; revised 18 November 2013; accepted 8 December 2013; published online 29 January 2014

achieve a specific strain to be reduced.<sup>6,9</sup> In our previous studies,<sup>10,11</sup> copper phthalocyanine oligomers (CuPc, Scheme 1) were used as a filler to enhance the dielectric constants of polymeric materials. CuPc, a planar, multiring organic semiconductor, exhibits a high dielectric constant ( $>10^5$ ) because of the electron delocalization within the large conjugated molecule.<sup>9–12</sup> As expected, when dispersed in a polymer matrix, the resulting composite exhibits an increased dielectric constant. In addition, as an organic material, CuPc has a modulus ( $\sim 2$  GPa) that is much smaller than that of its inorganic counterparts. Therefore, a high dielectric constant can be achieved in the resulting composites without sacrificing the flexibility of the polymeric materials.

It was observed, however, that blending also causes a decrease in the breakdown field and an increase in the dielectric loss of the resulting composites because of the agglomeration of CuPc into large spherical particulates ( $\sim 500$  nm). As a result, the size of the filler particles in composites, such as polymer/CuPc, must be substantially reduced. In our previous investigations, a grafting approach was used to reduce the CuPc particle size in the polymer matrix.<sup>10,11,13</sup> However, satisfactory dispersion of the CuPc particles was still not achieved. It should be particularly noted that, in these types of composites, the size of the CuPc particles dispersed in the polymer matrix has a significant impact because the filler–polymer interface has an important role in the enhancement of the dielectric response of the composites.<sup>14</sup>

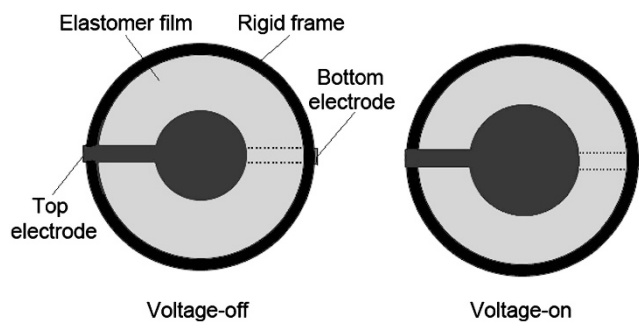
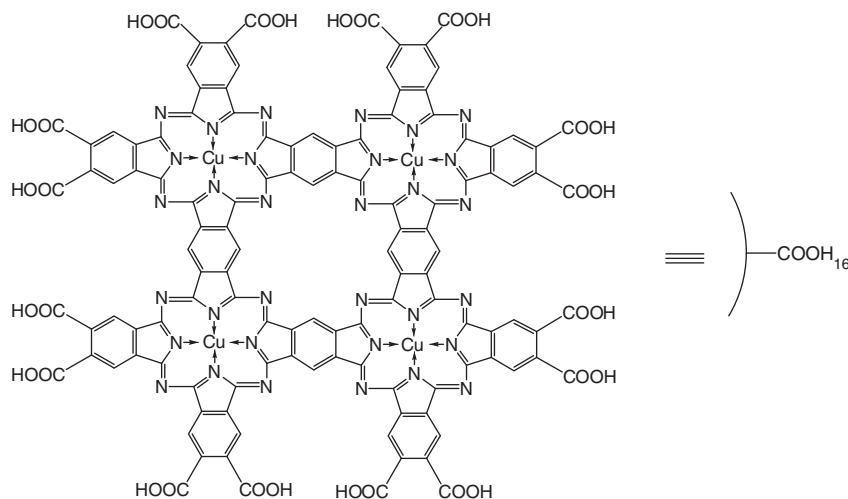


**Figure 1** Schematic illustration of a dielectric elastomer before and after the application of an external electrical potential across the film.



**Scheme 1** Chemical structure of the copper phthalocyanine oligomers (CuPc) oligomer; labels are shown on the right.

Motivated by the above considerations, we investigated the development of high dielectric constant elastomeric nanocomposites for electromechanical applications. Composites with different CuPc volume percentages or CuPc particle sizes were fabricated. PU was synthesized as the matrix because it is a ferroelectric polymer and exhibits excellent flexibility, and PU presenting isocyanate end groups can easily react with CuPc-containing carboxyl groups. The morphologies of these composites differ from each other, leading to unique dielectric responses. As will be noted later, by bonding CuPc oligomers to PU chains (referred to here as PU-CuPc), the dispersion of the oligomers in the PU matrix was remarkably improved, and for the resulting nanocomposite film with 8.78 vol% CuPc fabricated by a solution-cast technique with tailored morphology, an enhanced dielectric response was expected; a large electric field induced strain was achieved.

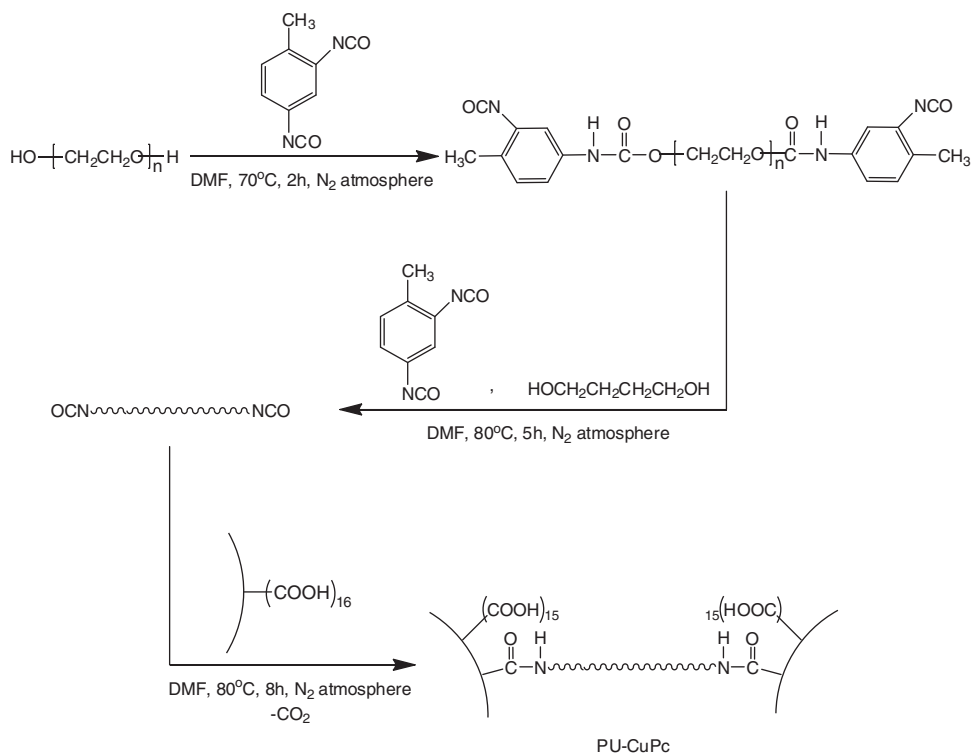
## EXPERIMENTAL PROCEDURE

### Materials

CuPc was synthesized following the procedure reported in Achar *et al.*<sup>15</sup> The soft segment, polyether N220 ( $M_n=2000$ ), was purchased from Nanjing Oswald Chemical Company (Nanjing, China), and was dehydrated and degassed under vacuum at 120 °C for 3 h and stored under dried nitrogen. The hard segment, 2,4-diisocyanatotoluene, was purchased from Shanghai BASF Polyurethane Co., Ltd. (Shanghai, China), distilled *in vacuo* and stored under dried nitrogen. Analytical grade 1,4-dihydroxybutane was dried with  $MgSO_4$  and then distilled under reduced pressure before use. Analytical grade dimethylformamide (DMF) was dried with  $CaH_2$ , distilled *in vacuo* and stored under dried nitrogen. All other chemicals were of analytical grade and were used as received.

### Preparation of PU-CuPc

The synthetic route for PU-CuPc is shown in Scheme 2. A 100 ml three-neck round-bottom flask fitted with a magnetic stirrer, an addition funnel, a condenser and a nitrogen inlet was used as the reactor. TDI (Tivoli Directory Integrator; 1.554 g, 8.93 mmol) was dissolved in 5 ml of DMF, added to the three-neck flask and stirred. N220 (5.0 g, 2.5 mmol) was dissolved in 15 ml of DMF and added to the funnel. The N220 solution was slowly (over approximately 0.5 h) dripped into the TDI solution. The reaction mixture was then stirred at 70 °C for 2 h under a purified nitrogen atmosphere to form the prepolymer. The prepolymer was then chain extended to form a high-molecular-weight polymer by adding 1,4-dihydroxybutane (0.54 g, 6.0 mmol) to the reaction mixture and stirring at 80 °C for 5.0 h. Next, a predetermined amount of CuPc dissolved in DMF (concentration 0.02  $g\ ml^{-1}$ ) was added to



**Scheme 2** Synthetic route for obtaining polyurethane-copper phthalocyanine oligomers (PU-CuPc).

the prepolymer solution through constant pressure drops from a liquid funnel. The solution was stirred at 80 °C for 8 h under a purified nitrogen atmosphere. The reaction mixture was precipitated into a large excess of distilled water. The resulting PU-CuPc was washed with methanol and dried under vacuum to a constant weight.

To obtain pure PU, the reaction mixture following chain extension was precipitated into a large excess of distilled water. The resulting PU was washed with methanol and dried under vacuum to a constant weight.

#### Preparation of films for mechanical and electric measurement

A solution-cast method was used to prepare the composite films. For the physical blends of PU and CuPc (termed PU/CuPc) containing different volume percentages of CuPc, a calculated amount of CuPc was added to the solution of PU in DMF, and the mixture was then ultrasonically stirred for approximately 2 h to obtain a homogeneous solution. Afterwards, the mixture was cast onto a polytetrafluoroethylene mold and dried in air at 70 °C for 12 h, followed by the thorough removal of solvent residue under vacuum at 70 °C for 12 h. Finally, the film was annealed at 120 °C in vacuum for 12 h and slowly cooled to room temperature (10 °C h<sup>-1</sup>).

To prepare the PU-CuPc films with varying CuPc contents, each composite was ultrasonically dissolved in DMF, and the same procedure used for the PU/CuPc films was then followed.

To fabricate composites with CuPc particulate sizes between those of PU/CuPc and PU-CuPc, PU-CuPc with a 1.26 or 3.58 vol% of CuPc and a correspondingly calculated amount of pure CuPc were ultrasonically dissolved in DMF and then submitted to the same procedure used for the PU/CuPc films. The total CuPc fraction of either composite was 8.78 vol%. The resulting nanocomposites were labeled PU-1.26CuPc/7.52CuPc and PU-3.58CuPc/5.20CuPc, respectively.

The typical film thickness is 80 μm.

#### Characterization

Fourier transform-infrared spectroscopy spectra were recorded with sample/KBr pressed pellets using a Vector-22 FT-IR spectrometer (Bruker AXS GmbH,

Karlsruhe, Germany). Inductively coupled plasma atomic emission spectrometry was used to determine the bonding ratio of CuPc in the PU-CuPc. Any unreacted CuPc in the samples was first removed by soaking the PU-CuPc in 50 ml of a 0.1 mol l<sup>-1</sup> NaOH aqueous solution followed by distilled water to remove the NaOH. The resulting product was dried *in vacuo* at 50 °C and then soaked in a crucible that contained a mixture of 3 ml of 70% nitric acid and 0.6 ml of 70% perchloric acid for 12 h. After evaporating all of the liquids in air at 80 °C, the organic components were burned in the crucible. The residues were diluted with 5% nitric acid to a 10 ml solution, and the metal contents were measured by a J-A1100 (Jarrell-Ash Co., Ltd., Waltham, MA, USA). TEM was performed using an H-7650 transmission electron microscope (Hitachi High-Technologies, Tokyo, Japan). The specimen was prepared by placing a drop of solution containing approximately 1.0 wt% of the composite in DMF on a carbon film-coated copper grid, and then drying with an infrared lamp in air before observation. The fracture surfaces of the composites fractured in liquid nitrogen were observed with an LEO 1550 field emission scanning electron microscope (LEO Elektronenmikroskopie GmbH, Oberkochen, Germany). The elastic moduli of the film samples with widths of 5 mm and lengths of 20 mm were determined with a dynamic mechanical thermal analyzer (Rheometric Scientific, Inc., Piscataway, NJ, USA; DMTA-V) at 1 Hz and room temperature. The selected amplitude of the dynamic deformation was 0.05%. An X-ray study was performed using a D8 Advance rotating anode X-ray generator (Bruker AXS GmbH, Karlsruhe, Germany) with a copper target. To characterize the frequency dependence of the dielectric properties, an Agilent 4194A precision impedance analyzer (Hewlett-Packard, Palo Alto, CA, USA) was used. The films for the test were cut into small pieces of 10 × 10 mm<sup>2</sup>, and circular gold electrodes with a 2.5 mm radius were sputtered in the center on both surfaces of each film sample. The dielectric constant  $K$  of the film was calculated using the formula for a parallel plate capacitor,  $K = Ct/\epsilon_0 A$ , where  $C$  is the capacitance of the capacitor,  $\epsilon_0$  is the vacuum dielectric permittivity ( $= 8.85 \times 10^{-12} \text{ F m}^{-1}$ ),  $A$  is the area of the electrode and  $t$  is the thickness of the capacitor. Strain measurements were made with the films stretched on a circular rigid frame. The bidirectional prestrain was 100%. Carbon-based conducting grease was brushed on the tops and bottoms of the films. A digital video optical system was used to measure

the lateral areal strain upon actuation. Measurements were collected approximately 1 s after application of the voltage. The corresponding transverse strain (along the specimen thickness direction) was computed from the measured lateral strain by assuming isochoric deformation and isotropic lateral displacement.

## RESULTS AND DISCUSSION

### Synthesis of PU-CuPc

To improve the compatibility between PU and CuPc and to substantially reduce the CuPc particle size in PU-CuPc, a sufficient quantity of CuPc should react with PU. Accordingly, to facilitate the reaction between the two components, it is advantageous for the PU chains to bear active functional groups that can easily react with the carboxyl groups on the CuPc molecules. To this end, PU end-capped with active -NCOs was synthesized. The Fourier transform-infrared spectroscopy spectra of CuPc, PU and PU-8.78CuPc ('8.78' represents the volume percentage (%) of CuPc) are shown in Figure 2. For PU-8.78CuPc, the absorption peak at  $1640\text{ cm}^{-1}$  corresponded to the stretching vibration of the carbonyl in the amide group (-NHCO-), the broad absorption band centered at approximately  $3406\text{--}3431\text{ cm}^{-1}$  corresponded to the N-H stretching vibration overlapped with the vibration of the O-H of the carboxyl group in CuPc, the bands centered at  $1721\text{ cm}^{-1}$  were because of the C=O stretching vibrations (free urethane C=O + C=O of carboxyl group) and the absorption bands in the range of  $920\text{--}931\text{ cm}^{-1}$  were attributed to -C-O-C- non-symmetric stretching overlapped with the vibrations of the coordinate bonds between the copper ion and the nitrogen atoms in each pyrrole ring in CuPc. These peaks indicate that the CuPc oligomers were successfully bonded to the PU chains. The peaks in the range of  $2974\text{--}2869\text{ cm}^{-1}$  were assigned to the C-H symmetrical and asymmetrical stretching absorptions of the CH<sub>3</sub> and CH<sub>2</sub> groups, while the other CH<sub>2</sub> vibration modes were manifested by the bands at  $1450, 1413, 1373$  and  $1300\text{ cm}^{-1}$ . The shoulder at  $1690\text{ cm}^{-1}$  was due to the hydrogen-bonded urethane C=O group. The bands at  $1598$  and  $1470\text{ cm}^{-1}$  are characteristic of benzene rings. The absorption bands from urethane N-H bending and C-N stretching were located at  $1535\text{ cm}^{-1}$ . The NCO peak at approximately  $2270$  was absent, suggesting that the NCO groups had completely reacted with the carboxyl groups of CuPc. According to the inductively coupled plasma atomic emission spectrometry analysis, it

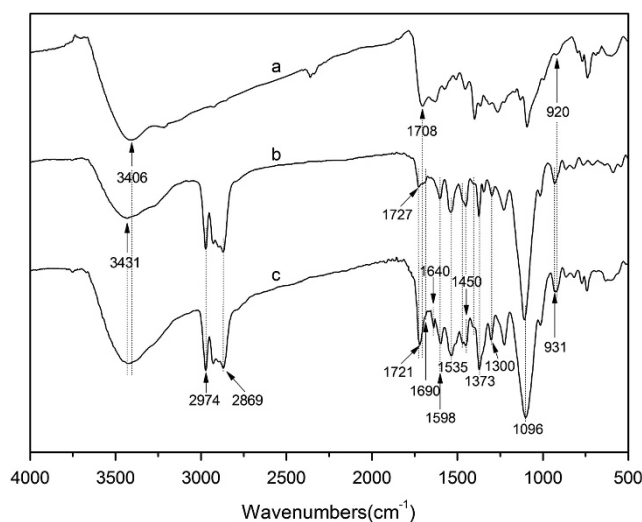


**Figure 2** Fourier transform-infrared spectroscopy (FT-IR) spectra of (a) copper phthalocyanine oligomers (CuPc), (b) polyurethane (PU) and (c) PU-8.78CuPc.

was estimated that the chemically bonded CuPc in the synthesized PU-8.78CuPc was as high as 96.8%.

### Microstructure of the composites

To investigate the influence of the CuPc particle size on the dielectric properties of the composites, composites with varying CuPc particle sizes were fabricated by different methods. TEM micrographs of PU/8.78CuPc, PU-1.26CuPc/7.52CuPc, PU-3.58CuPc/5.20CuPc and PU-8.78CuPc are illustrated in Figure 3. It is evident that the dispersion of CuPc varies in the four composites. For PU/8.78CuPc, because of the incompatibility of CuPc with PU, the CuPc molecules aggregated into nearly spherical particles approximately 250–600 nm in diameter in the polymer matrix (Figure 3a). This behavior was likely due to the strong tendency of CuPc to form stack assemblies and microaggregates due to its planar shape and aromatic nature.<sup>10</sup> Within the PU-8.78CuPc sample, the CuPc inclusions exhibited average diameters in the range of 10–20 nm (Figure 3d), much smaller than those of the particles in PU/8.78CuPc, which were dispersed in the PU matrix. This observation can be attributed to the fact that in PU-8.78CuPc, a portion of the CuPc oligomers attached to the PU can act as nucleation centers to further induce the growth of CuPc oligomer crystallites. However, because the mobility of the bonded CuPc groups was hindered by the PU backbone, the accessibility of the adjacent CuPc molecules was restricted, and the growth of crystallites was markedly limited. In contrast, the aggregation of CuPc readily occurred in PU/8.78CuPc.

Furthermore, within PU-1.26CuPc/7.52CuPc and PU-3.58CuPc/5.20CuPc, the sizes of the CuPc particulates ranged from 50 to 150 nm (Figure 3b) and 30–70 nm (Figure 3c), respectively, and were much larger than those in PU-8.78CuPc but much smaller than those in PU/8.78CuPc. This can be attributed to the fact that in the two PU-CuPc/CuPc samples including bonded and blended CuPc, the presence of PU-CuPc enhances the compatibility between PU and CuPc. Consequently, the CuPc particle size was remarkably lower than that in PU/8.78CuPc.<sup>13,16</sup> Nevertheless, the blended CuPc molecules in PU-CuPc/CuPc can move more easily toward nucleation centers than the chemically bonded molecules can. Therefore, compared with PU-8.78CuPc, the two PU-CuPc/CuPc samples included larger-sized CuPc particles. The content of bonded CuPc in PU-1.26CuPc/7.52CuPc was lower than that in PU-3.58CuPc/5.20CuPc, indicating that the compatibility between PU and CuPc in PU-1.26CuPc/7.52CuPc was inferior to that in PU-3.58CuPc/5.20CuPc. As a result, the CuPc particle size in the former was larger than that in the latter. It should be noted that smaller CuPc particle sizes increase the interface exchange coupling effect. This phenomenon will be explained in greater detail in the next section.

As can also be observed in Figure 3, the four composites display different CuPc particulate morphologies. With an increase in the chemically bonded CuPc content in the composites, the shapes of the CuPc particulates changes from nearly spherical in shape to irregular in shape. For example, the shape of the CuPc particulates in PU-8.78CuPc was irregular (Figure 3d). In contrast, in PU/8.78CuPc, the CuPc molecules aggregated into nearly spherically shaped particles (Figure 3a). During the phase separation between PU and CuPc as the minor component, which is driven by a reduction in the surface energy of the CuPc particulates, the oligomers spontaneously formed spherically shaped particles upon solvent evaporation in the PU/8.78CuPc blend. In the PU-8.78CuPc sample, however, because the movement of the bonded CuPc molecules was obstructed by

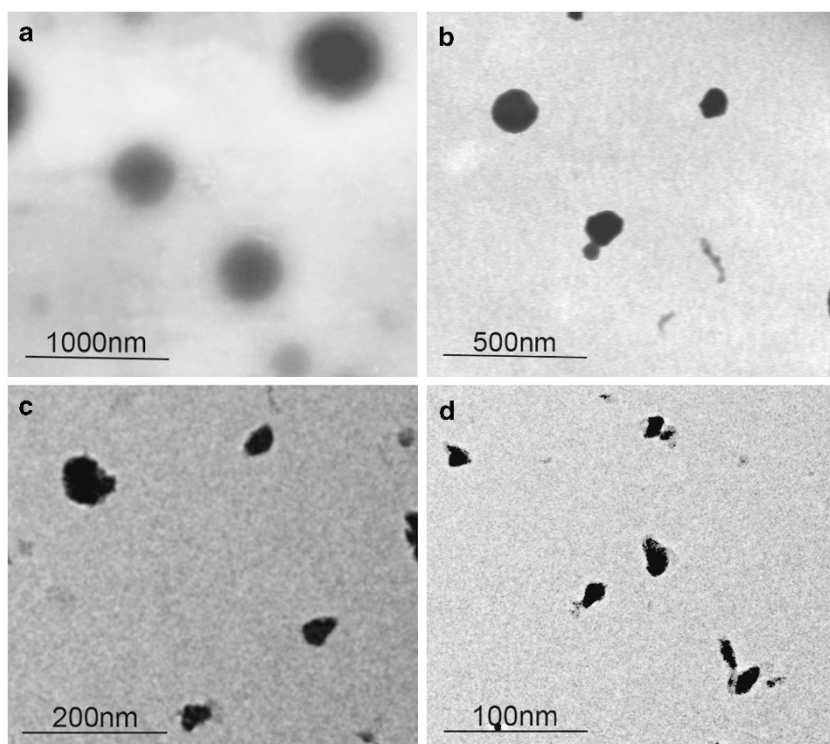


**Figure 3** Transmission electron microscope (TEM) pictures of (a) polyurethane (PU)/8.78CuPc, (b) PU-1.26CuPc/7.52CuPc, (c) PU-3.58CuPc/5.20CuPc and (d) PU-8.78CuPc. CuPc, copper phthalocyanine oligomers.

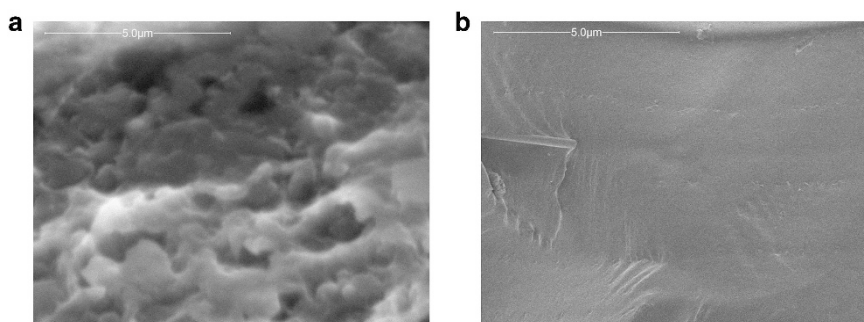


**Figure 4** Scanning electron microscope (SEM) photographs of the fracture surfaces of films of (a) polyurethane (PU)/8.78CuPc and (b) PU-8.78CuPc. CuPc, copper phthalocyanine oligomers.

the PU chains, they were unable to move freely and form spherical crystallites.

To further compare the dispersion of CuPc in PU/8.78CuPc and PU-8.78CuPc, field emission scanning electron microscope was used to observe the fracture surfaces of the film specimens. It is apparent in Figure 4a that in the PU/8.78CuPc sample, aggregates of CuPc particulates were present in the polymer matrix. In contrast, PU-8.78CuPc exhibited a homogeneous structure under a magnification of  $\times 4000$ , and no inclusion phases could be observed (Figure 4b). These results reveal that the chemical bonding of the CuPc oligomers to the PU chains can indeed improve the compatibility of the two components. Furthermore, the aggregation of oligomers can be difficult to prevent in the physical blend, which is in good agreement with the results of TEM analysis.

The XRD patterns of PU, PU/8.78CuPc and PU-8.78CuPc acquired at room temperature are shown in Figure 5. The pure PU and

composite samples show diffuse X-ray peaks at  $20^\circ$  in  $2\theta$ , indicating the amorphous nature of polyurethane, in agreement with previous work. However, a short-range residual order of PU chain segments was observed.<sup>17</sup> In addition, by comparing the two composites, it was found that the magnitudes of the peaks at  $20^\circ$  were much lower than those of the neat PU sample because the introduction of CuPc molecules handicapped the orientation of the segments, hindering their orderly arrangement. For the composites, the diffraction peak at  $27^\circ$  in  $2\theta$  that had a corresponding d-spacing that was 3.30 Å arose from the CuPc crystalline phase in the PU matrix, explaining the absence of this peak in the pure PU. Note that the intensity of the peak at  $27^\circ$  for PU/8.78CuPc was much stronger compared with that of PU-8.78CuPc. This suggests that the crystallinity of CuPc in PU-8.78CuPc was much lower than that in PU/8.78CuPc, because the mobility of the bonded CuPc molecules was restrained by the PU chains.

The elastic moduli were measured to be 21.7 and 29.6 MPa in ambient conditions for the pure PU and the PU-8.78CuPc, respectively. In PU-CuPc, the bonded CuPc molecules formed crystallites that acted as physical crosslinking points with an elastic modulus ( $\sim 2$  GPa) much higher than that of the PU matrix. This effect will inevitably result in a higher elastic modulus for PU-CuPc compared with pure PU.<sup>18</sup>

### Dielectric properties of the composites

Figure 6a shows the dielectric constants of PU-CuPc and PU/CuPc measured at 100 Hz as a function of the volume fraction of CuPc together with the curve calculated from Equation (1). Figure 6b presents the dielectric constants at 100 Hz of PU and the composites containing 8.78 vol% CuPc together with the calculated value from

Equation (1). As expected, the dielectric constants increase with increasing CuPc volume fraction. It should be noted that the dielectric constants of the composites were much higher than those derived from the various models, especially for the PU-CuPc sample. For instance, if we regard the composites as random mixtures of the PU matrix and CuPc particulates, according to the widely used logarithmic dielectric mixing rule proposed by Lichtenecker and co-workers,<sup>3</sup> the effective dielectric constant ( $K$ ) of the composites can be estimated as:<sup>3</sup>

$$\ln K = c_1 \ln K_1 + c_2 \ln K_2 \quad (1)$$

where  $K_1$  and  $K_2$  are the dielectric constants of the dielectric filler and the polymer matrix, respectively, and  $c_1$  and  $c_2$  are the volume fractions of the filler and matrix, respectively. Here,  $K_1$  and  $K_2$  at 100 Hz are  $4.3 \times 10^5$  and 6.3, respectively. Obviously, as illustrated in Figures 6a and b, this model cannot be used to explain the large enhancements in the dielectric constants observed in the composites, especially for those containing chemically modified CuPc. The enhancements in the dielectric constants of the composites may therefore arise primarily from the interface effect.<sup>14</sup> We will discuss this aspect later.

The frequency-dependent dielectric constant and dielectric loss at room temperature from 100 to 100 kHz are shown in Figure 7 for both the pure PU and the four composites (PU-8.78CuPc, PU-1.26CuPc/7.52CuPc, PU-3.58CuPc/5.20CuPc and PU/8.78CuPc). As expected, the dielectric constants of the composites are much higher than those of the pure PU (Figure 7a). For instance, at 100 Hz, the dielectric constants of PU-8.78CuPc, PU-3.58CuPc/5.20CuPc, PU-1.26CuPc/7.52CuPc and PU/8.78CuPc are 391, 310, 102 and 48, respectively, representing enhancements of approximately 62-, 49-, 16- and 7.4-fold with respect to the dielectric of the pure PU, respectively. In addition, for each composite sample, dielectric dispersion at low frequencies was observed. This phenomenon is ascribed to the interfacial polarization (Maxwell–Wagner polarization) mechanism caused by the large difference between the dielectric constants of the polymer matrix and the filler.<sup>19–21</sup>

Interestingly, as observed in Figure 7a, although the CuPc content in the four composite samples was the same, with either increasing

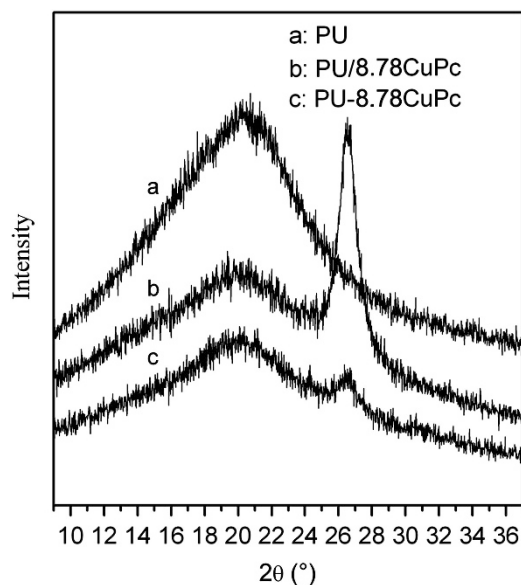


**Figure 5** X-ray data from (a) polyurethane (PU), (b) PU/8.78CuPc and (c) PU-8.78CuPc. CuPc, copper phthalocyanine oligomers.

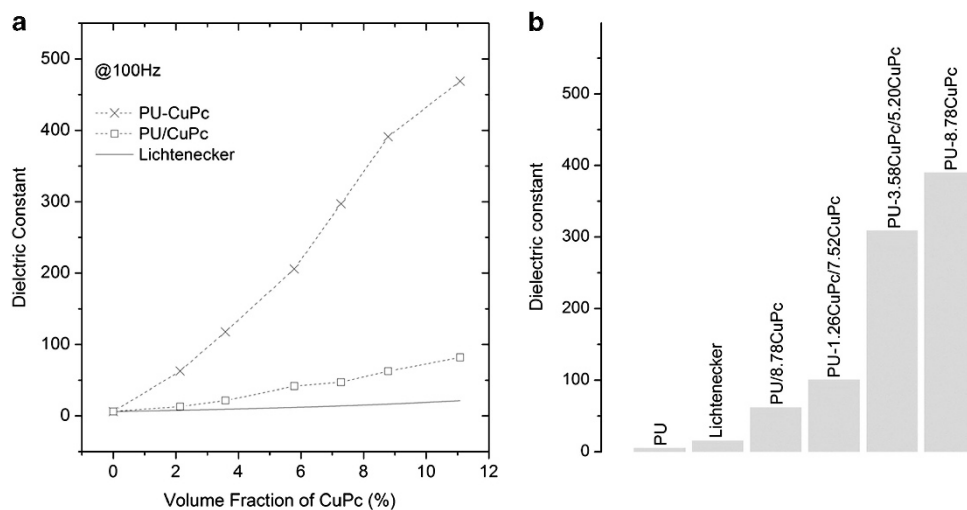


**Figure 6** (a) Variations in the dielectric constants of polyurethane-copper phthalocyanine oligomers (PU-CuPc) and PU/CuPc containing a volume fraction of CuPc measured at room temperature and 100 Hz. The dashed curves are a guide to the eye, and the solid curve was calculated from Equation (1). (b) Dielectric constants (100 Hz) of PU and the composites containing 8.78 vol% CuPc plotted along with the calculated value from Equation (1).

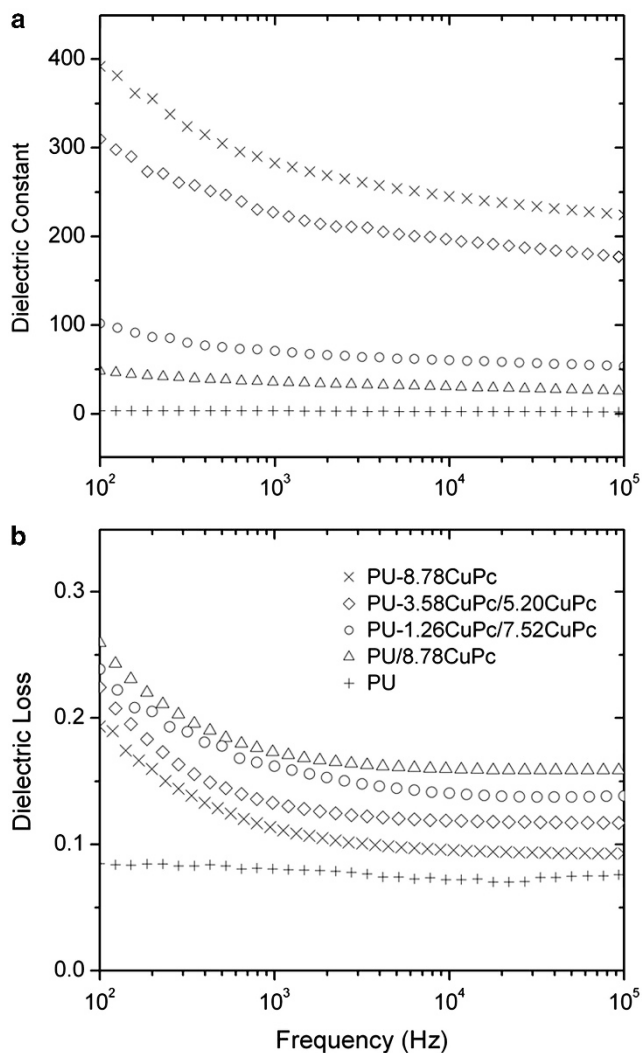


**Figure 7** Dielectric constant (a) and dielectric loss (b) versus frequency from 100 to 100 kHz at room temperature for pure polyurethane (PU), PU/8.78CuPc, PU-1.26CuPc/7.52CuPc, PU-3.58CuPc/5.20CuPc and PU-8.78CuPc. CuPc, copper phthalocyanine oligomers.

chemically bonded CuPc content or decreasing CuPc particle size (see Figure 3), the dielectric constants of the composites from PU/8.78CuPc to PU-8.78CuPc increased substantially. It was suggested that this phenomenon was caused by the interface exchange coupling effect. Li<sup>14</sup> predicted that for a composite-like polymer with a high dielectric constant filler, as the heterogeneity in the composite decreases, the influence of the exchange layer, an interface layer in which the polarization is strongly affected by both phases, becomes increasingly important and eventually dominates when the heterogeneity size and the exchange length become comparable. Therefore, the marked enhancement of the dielectric response observed in PU-8.78CuPc was most likely caused by the stronger exchange coupling effect as well as the interfacial polarization effect due to the much smaller CuPc particle size in PU-8.78CuPc compared with the other composite samples, as observed in the TEM micrographs.

As presented in Figure 7b, the dielectric losses of the composites were relatively low. CuPc suffered a high dielectric loss because of the long-range intermolecular hopping of electrons.<sup>12,13</sup> In the compo-

sites, the polymer matrix acted as an insulation layer to significantly reduce the dielectric loss of CuPc. Over the frequency range observed in Figure 7b, the loss of the PU-8.78CuPc was lower than those of the other composites, which can be attributed to the reduced particle size and improved dispersion of CuPc in PU-8.78CuPc. The loss of the PU-8.78CuPc at 100 Hz is approximately 0.19.

Owing to the large dielectric response in PU-8.78CuPc, the field-induced thickness strain ( $S$ ) of the PU-8.78CuPc film reached 17.7% under an electric field of  $10 \text{ V } \mu\text{m}^{-1}$ . Assuming that the composites discussed here are linear elastic materials, the stored elastic energy ( $E_s$ ) can be written as:  $E_s = YS^2/2$ , where  $Y$  is the elastic modulus of the composite. Combining the strain and elastic modulus (29.6 MPa) data yielded an elastic energy density of  $0.927 \text{ J cm}^{-3}$  for PU-8.78CuPc under  $10 \text{ V } \mu\text{m}^{-1}$ . In comparison, under the same driving field, the induced strain from PU/8.78CuPc was 3.3%. The elastic modulus of PU/8.78CuPc was 21.7 MPa, which yielded a  $0.024 \text{ J cm}^{-3}$  elastic energy density for the simple blend. These results indicate that the strain of PU-8.78CuPc increased nearly 5.4-fold compared with that of the PU/8.78CuPc sample and that the elastic energy density of PU-8.78CuPc was enhanced more than 38-fold compared with that of PU/8.78CuPc.

Its large strain, high elastic energy density, low loss and good flexibility make PU-8.78CuPc very attractive in current electromechanical applications.

## CONCLUSION

Nanocomposites of PU with chemically bonded and/or blended CuPc oligomers were investigated. The sizes of the CuPc particles within the nanocomposite containing 8.78 vol% bonded CuPc ranged from 10 to 20 nm. The particle size had an important role in the enhancement of the electric performance of the nanocomposite. The nanocomposite exhibited a high dielectric constant (391; more than 60-fold greater than that of the pure elastomer matrix and more than 8-fold greater with respect to that of the simple blend), low loss (0.19), large electric field induced strain (17.7% under  $10 \text{ V } \mu\text{m}^{-1}$ ) and a high elastic energy density ( $0.927 \text{ J cm}^{-3}$ ), all of which are highly desirable for high-performance electromechanical actuators and artificial muscles.

## ACKNOWLEDGEMENTS

This work was supported by the National Natural Science Foundation of China (No. 21174063), the Natural Science Foundation of Jiangsu Province (No. BK20131358) and the Aeronautical Science Foundation of China (No. 2011ZF52063).

- 1 Stoyanov, H., Brochu, P., Niu, X. F., Lai, C., Yuna, S. & Pei, Q. B. Long lifetime, fault-tolerant freestanding actuators based on a silicone dielectric elastomer and self-clearing carbon nanotube compliant electrodes. *RSC Adv.* **3**, 2272–2278 (2013).
- 2 Huang, J. H., Shian, S., Suo, Z. G. & Clarke, D. R. Maximizing the energy density of dielectric elastomer generators using equi-biaxial loading. *Adv. Funct. Mater.* **23**, 5056–5061 (2013).
- 3 Stoyanov, H., Kollasche, M., Risse, S., McCarthy, D. N. & Kofod, G. Elastic block copolymer nanocomposites with controlled interfacial interactions for artificial muscles with direct voltage control. *Soft Matter.* **7**, 194–202 (2011).
- 4 Bozlar, M., Puncck, C., Korkut, S., Zhu, J., Foo, C. C., Suo, Z. G. & Aksay, I. A. *Appl. Phys. Lett.* **101**, 091907-1–091907-5 (2012).
- 5 Anderson, I. A., Gisby, T. A., McKay, T. G., O'Brien, B. M. & Calius, P. Multi-functional dielectric elastomer artificial muscles for soft and smart machines. *J. Appl. Phys.* **112**, 041101-1–041101-20 (2012).
- 6 O'Halloran, A., O'Malley, F. & McHugh, P. A review on dielectric elastomer actuators, technology, applications, and challenges. *J. Appl. Phys.* **104**, 071101-1–071101-10 (2008).
- 7 Pelrine, R., Kornbluh, R., Pei, Q. B. & Joseph, J. High-speed electrically actuated elastomers with strain greater than 100%. *Science* **287**, 836–839 (2000).

- 8 Kornbluh, R., Heydt, R. & Pelrine, R. in *Biomedical Applications of Electroactive Polymer Actuators* (eds Carpi, F. & Smela, E.) Ch. 20 387–392 (Wiley, New York, NY, USA, 2009).
- 9 Zhang, Q. M., Li, H. F., Poh, M., Xu, H. S., Cheng, Z. Y., Xia, F. & Huang, C. An all-organic composite actuator material with a high dielectric constant. *Nature (London)* **419**, 284–287 (2002).
- 10 Wang, J. W., Wang, Y., Wang, F., Li, S. Q., Xiao, J. & Shen, Q. D. A large enhancement in dielectric properties of poly(vinylidene fluoride) based all-organic nanocomposite. *Polymer (Guildf)* **50**, 679–684 (2009).
- 11 Wang, J. W., Wang, Y., Li, S. Q. & Xiao, J. Enhanced dielectric response in P(VDF-TrFE) based all-organic nanocomposites. *J. Polym. Sci. Part B* **48**, 490–495 (2010).
- 12 Nalwa, H. S., Dalton, L. R. & Vasudevan, P. Dielectric properties of copper-phthalocyanine polymer. *Eur. Polym. J.* **21**, 943–947 (1985).
- 13 Wang, J. W., Shen, Q. D., Bao, H. M., Yang, C. Z. & Zhang, Q. M. Microstructure and dielectric properties of P(VDF-TrFE-CFE) with partially grafted copper phthalocyanine oligomer. *Macromolecules* **38**, 2247–2252 (2005).
- 14 Li, J. Y. Exchange coupling in P(VDF-TrFE) copolymer based all-organic composites with giant electrostriction. *Phys. Rev. Lett.* **90**, 217601-1–217601-4 (2003).
- 15 Achar, B. N., Fohlen, G. G. & Parker, J. A. Phthalocyanine polymers. II. Synthesis and characterization of some metal phthalocyanine sheet oligomers. *J. Polym. Sci.* **20**, 1785–1790 (1982).
- 16 Wang, J. W., Shen, Q. D., Yang, C. Z. & Zhang, Q. M. High dielectric constant composite of P(VDF-TrFE) with grafted copper phthalocyanine oligomer. *Macromolecules* **37**, 2294–2298 (2004).
- 17 Ma, J., Liu, C. H., Li, R., Wu, H. X., Zhu, L. N. & Yang, Y. J. Preparation and properties of castor oil-based polyurethane/a-zirconium phosphate composite films. *J. Appl. Polym. Sci.* **121**, 1815–1822 (2011).
- 18 Huang, C., Zhang, Q. M., DeBotton, G. & Bhattacharya, K. All-organic dielectric-percolative three-component composite materials with high electromechanical response. *Appl. Phys. Lett.* **84**, 4391–4393 (2004).
- 19 Seanor, D. A. *Electrical Properties of Polymers* (Academic Press, New York, NY, USA, 1982).
- 20 Bobnar, V., Levstik, A., Huang, C. & Zhang, Q. M. Distinctive contributions from organic filler and relaxorlike polymer matrix to dielectric response of CuPc-P(VDF-TrFE-CFE) composite. *Phys. Rev. Lett.* **92**, 047604-1–047604-4 (2004).
- 21 Bobnar, V., Levstik, A., Huang, C. & Zhang, Q. M. Dielectric properties and charge transport in all-organic relaxorlike CuPc-P(VDF-TrFE-CFE) composite and its constituents. *Ferroelectrics* **338**, 107–116 (2006).